

A STUDY OF FLOW AND INITIAL STAGE OF WATER CONDENSATION IN THE TWO-PHASE JET-VORTEX WAKE BEHIND A CRUISE AIRCRAFT

Maria A. Lobanova

**Department of Plasma and Gas Dynamics and Heat Engineering
Baltic State Technical University**

Key words: *cruise, jet-vortex wake, exhaust jet, water clusters*

Abstract

The paper describes the results of numerical investigation of large-scale flow structure in the near aircraft wake on the basis of Reynolds Averaged Navier-Stokes equations. Influence of computational domain decomposition, grid refinement and the flow model on the jet flow field is analyzed. Initial growth of water clusters in the exhaust jet and the cluster distribution in size are studied at different distance from the nozzle outlet.

1 Introduction

Being an essential and integral element of nowadays global society, aviation is still a field of growing scientific interest, particularly because of its impact on environmental conditions. Recent years are described by trends in setting highly ambitious goals in developing and creating environmentally friendly air vehicles and new transport infrastructure [1]. High-profile questions in this focus area and new large scale simulation strategies for greener technologies are widely discussed among both scientists and politicians. Good example is Clean Sky, one of the most ambitious aeronautical research programme launched in Europe [2]. Its mission is to develop breakthrough technologies to significantly decrease the effect of air transport on the environment.

No less important is flight safety control both in airport area and along flight corridors. It is known, that aircraft during flight leaves behind it a strongly disturbed vortex sheet

formed from flow around wings and interacting with exhaust jets. This area is known as a jet-vortex wake. A difference of vertical velocity component across the wake can reach the level of more than 25 m/s, which presents a significant danger for aircrafts, going the same flight corridor. According to current flight rules in order to prevent emergency situations airplanes takeoff and land with scheduled time interval, avoiding aircraft entering a jet-vortex wake of another aircraft. Arising in the process of condensation water aerosol (water droplets and ice crystals) can act as a marker for the jet-vortex wake visualization and characterization with optical methods and, as a consequence, for the vortex danger estimation. This problem can be of great importance for metropolis airports with high-density air traffic.

Besides a jet-vortex wake of great interest is so-called condensation trail (contrail), resulting from condensation of water vapour, containing in the products of aviation fuel combustion and in the atmosphere. Such contrails provide formation of artificial clouds that disrupts the local heat balance in the atmospheric boundary layer. While studying contrail properties, a problem of jet-vortex wake modeling is one of the most important, because the physical-chemical processes in the jet and in the atmosphere occur against a background of complex gas-dynamic structure of the wake.

The objective of this work is numerical study of the jet-vortex wake in general and, particularly, exhaust jets, as well as the study of the initial stage of water clusters formation in the products of fuel combustion.

2 Numerical simulation of the jet-vortex wake

2.1 Geometric configuration of an aircraft

To construct a three-dimensional geometric aircraft model, its configuration and sizes were taken as for the B737-300 aircraft, available in the open information sources [3]. Airfoil coordinates in different wing's cross-sections were borrowed from the Illinois airfoil database (Chicago, USA) [4]. The aircraft configuration included fuselage, wings (with and without winglets), turbofan engine nacelles, horizontal and vertical stabilizers, nacelle pylons, and flap track fairings. The aircraft 3D-configuration was designed using SolidWorks soft, and it is shown in Fig. 1.



Fig. 1. Aircraft configuration in computational simulation.

The fuselage length was 32.18 m, its height and width in the middle part were 4.01 m и 3.76 m respectively, wing span was

31.20 m with and 28.88 m without winglets, wing dihedral was 6° , horizontal stabilizer span was 12.7 m, horizontal stabilizer dihedral was 7° , angle between the root airfoil chord and the fuselage centerline (setting angle) was $+1^\circ$, the wing was geometrically twisted and the setting angle for wing tips was -0.8° . The horizontal stabilizers have no geometrical twisting and their setting angle was -2° . The length of engine nacelle was 4.0 m. The diameters of the annular exhaust duct and bypass duct outlets were 0.51 m and 0.76 m, and 1.04 m and 1.30 m, respectively. The aircraft attack angle during cruise flight was 5° .

2.2 Flow model description

To simulate the large-scale flow structure of the jet-vortex wake RANS approach was used. Contrary to other methods, developed to resolve the most small eddies (for example, Large Eddy Simulation (LES) or Direct Numerical Simulation (DNS)), RANS approach doesn't need very fine grid, however it allows to simulate the large-scale vortex flow structure and mixing layers with high accuracy and is widely used in engineering applications.

In our research Reynolds Averaged Navier-Stokes equations were closed with the Menter $k - \omega$ SST turbulence model [5]. This turbulence model gives good agreement with the experimental data in drag and lift force coefficients for the simplified model configurations of an aircraft (wing/fuselage and wing/fuselage/nacelle/pylon) [6] and has been widely used for many years in engineering calculations of leading aviation companies.

2.3 Calculation domain, grid and boundary conditions

The calculation domain represented a rectangular parallelepiped (see Fig. 2) 160.91 m in length (5 fuselage lengths), 46.62 m width (wing semispan plus fuselage length), and 64.36 m height (2 fuselage lengths). The flow was assumed to be symmetric relative to the vertical plane passing through the aircraft centerline. In Fig. 2 the axes orientation is presented. The origin of

coordinates is located in the plane of symmetry (x -axis is measured from this plane) at equal distance from the top and bottom boundaries and at a distance 28.88 m from the inlet boundary.

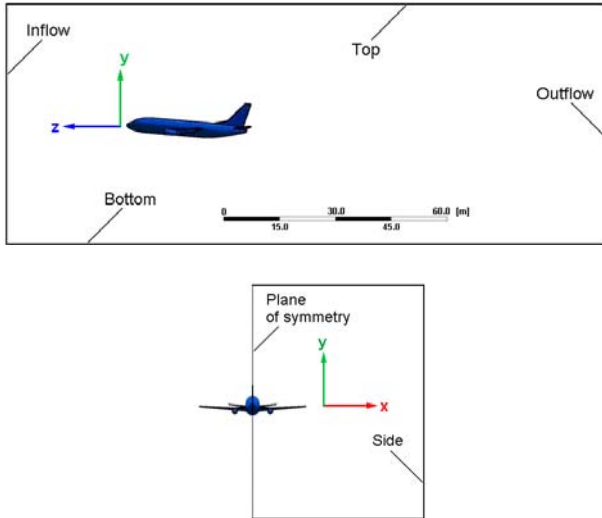


Fig. 2. Calculation domain in (yz)- and (xy)-planes and aircraft position.

Unstructured grid with 19 million cells was designed using the ANSYS ICEM CFD soft. Special attention was given to grid refinement on wing tips, and the area of vortex sheet and exhaust jets flow propagation. Such domain decomposition is of particular importance for further calculations of water vapour condensation in the wake.

The temperature and the total pressure corresponded to the free stream parameters ($V = 216$ m/s – speed of flight, static pressure $p = 26607.8$ Pa and temperature $T = 223.15$ K at the height of 10 km) were specified at the inlet boundary.

At the outlet boundary free stream pressure was imposed, all other parameters were extrapolated from the calculation domain. As the boundary conditions at the top, bottom and side boundaries the velocity vector and the temperature as in the free stream were specified ($V_x = 0$, $V_y = 0$, $V_z = -216$ m/s, $T = 223.15$ K).

On the aircraft surface, flow tangency conditions together with the “no-slip wall” and adiabatic conditions were imposed.

Parameters of flow at the exhaust and bypass duct outlets were determined from the

thermodynamic calculations for the turbofan engine CFM 56-3. The velocity and static temperature values were found to be equal to 517.37 m/s and 366.86 m/s, and 883.36 K and 236.4 K, respectively. The turbulence intensity was taken 5 %. For simplicity, the gas constant and the ratio of specific heats for combustion products were taken identical to those for air.

The conditions of symmetry were specified at the plane of symmetry: the normal velocity (x -component) and all derivatives of thermodynamic parameters and y - and z -components of the velocity vector with the respect to the normal direction (x -direction) were zero.

The free stream velocity vector, temperature and pressure were taken as the initial conditions in the whole calculation domain.

More detailed information about calculation domain, grid and boundary conditions is given in [7].

2.4 Numerical results

All calculations are done using ANSYS CFX soft.

In Fig. 3, the view of streamlines in the jet-vortex wake flow behind the aircraft is shown. Vortex sheet flowing from wing tips is rolling up, forming two large vortices. It is interesting to note that jets do not intersect the vortex sheet, but they are only drawn in it, and, hence, not directly interact with the sheet.

In Fig. 4, the velocity and vorticity fields in the outlet boundary of the calculation domain ($z = -130$ m) are presented. The maximal value of the xy -component of the vorticity vector (in Fig. 4 $VCurl_{XY} = ((Curl_x)^2 + (Curl_y)^2)^{1/2}$) is observed in the jets.

The dependence of the vertical velocity component on x -coordinate at $y = -1.30$ m and different z for aircraft with and without winglets is shown in Fig. 5.

Comparison of functions $V_y(x)$ in the wake is in good agreement with the well-known fact that winglets decrease the vortex drag of an aircraft. At the same time it should be noticed that contrary to the wide-spread

point of view, winglets almost play no role in formation of the circulation flow at wing tips.

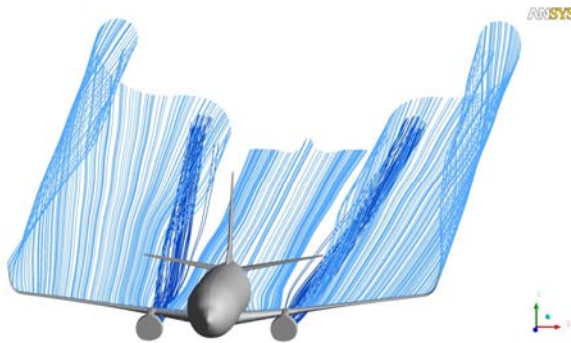


Fig. 3. View of streamlines in the jet-vortex wake.

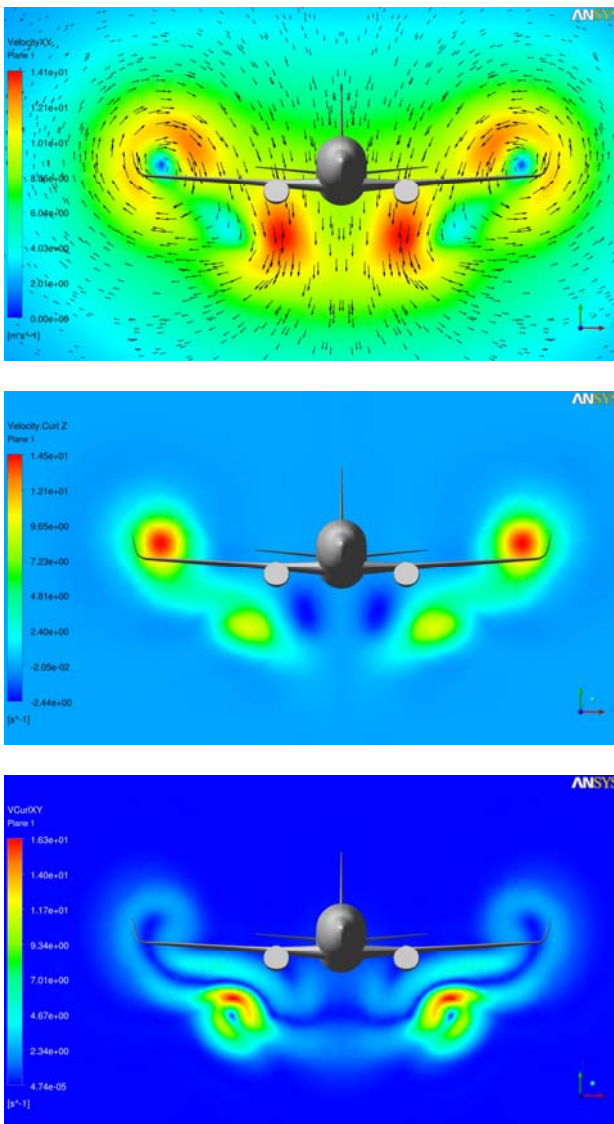


Fig. 4. Fields of velocity in (xy)-plane (top), z-component of the vorticity vector (centre), and the vorticity vector component in the (xy)-plane (bottom).

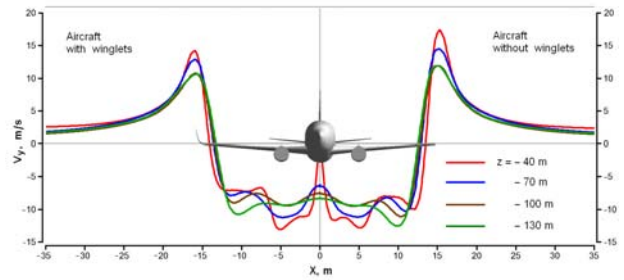


Fig. 5. Vertical velocity component in different cross-sections of the wake along the line $y = -1.3$ m: for an aircraft with (left) and without (right) winglets.

3 Numerical simulation of the turbofan engine exhaust jet flow

The aim of this research was to estimate the influence of the degree of calculation domain decomposition on fields of the gas-dynamic parameters in the jet. As is well known, grid used in computational simulation has a strong influence on the accuracy of numerical solution, in particular, on the temperature distribution along and across the jets, which is important for further calculations of water condensation. Finding grid settings, providing an acceptable accuracy of the turbofan engine jet flow field with a relatively small number of grid cells, is of great importance for numerical simulation of the whole of flow around an aircraft and in the jet-vortex wake behind it, which requires at least an order of magnitude greater number of cells.

3.1 Calculation domain, initial and boundary conditions

As a part of general study of jet-vortex wake modeling (section 2) the flow of a single jet of a turbofan engine is considered below. All dimensions of the the exhaust and bypass duct outlets were assumed as in the section 2.1.

The calculation domain represented a cylinder with 7.14 m diameter and 55.74 m length that approximately corresponds to 9 and 53 external diameters of the annular exhaust duct outlet. The coordinates are positioned so that the stream flows against the z -axis. The y -axis is directed upwards, the x -axis is normal to the (yz)-plane. The origin of coordinates coincides with the center of the circular inlet

A STUDY OF FLOW AND INITIAL STAGE OF WATER CONDENSATION IN THE TWO-PHASE JET-VORTEX WAKE BEHIND A CRUISE AIRCRAFT

boundary of the computational domain and at the same time belongs to the symmetry axis of the exhaust and bypass nozzles.

Jet stream was simulated using three structured block grids with the number of cells of 1, 6 and 10 million. Fig. 6 shows an example of a one million cells grid. Discretization of the computational domain was adapted to the geometry of the nozzles of both ducts and flow characteristics, in particular, to strongly gradient flow at the nozzle exit and in the jet. Annular nozzles outlets have good radial resolution of 25 cells.

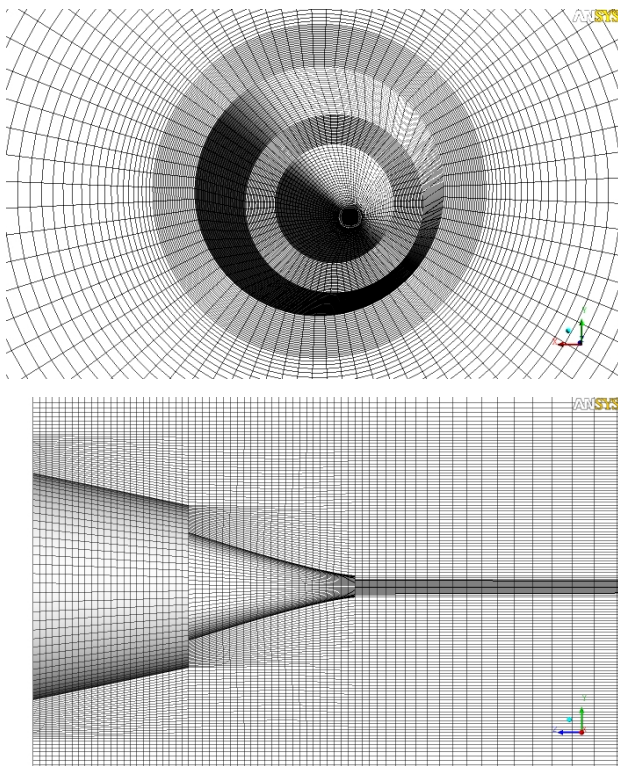


Fig. 6. View of a grid with one million cells.

Reynolds Averaged Navier-Stokes equations were solved numerically with the use of the Menter $k-\omega$ SST turbulence model.

At the exhaust and bypass duct outlets temperature and pressure were specified (883.36 K and 236.4 K, and 517.37 m/s and 366.86 m/s, respectively).

The angle of inclination of the velocity vector at the exhaust and bypass duct exits was varied so that the velocity vector was tangent to the corresponding wall of the nozzle (Fig.7). This way of setting of the boundary conditions allowed avoiding flow separation immediately

behind the nozzle and appearance of the vacuum and circulation flow areas, which were obtained in the case of setting the normal to the boundary velocity vector.

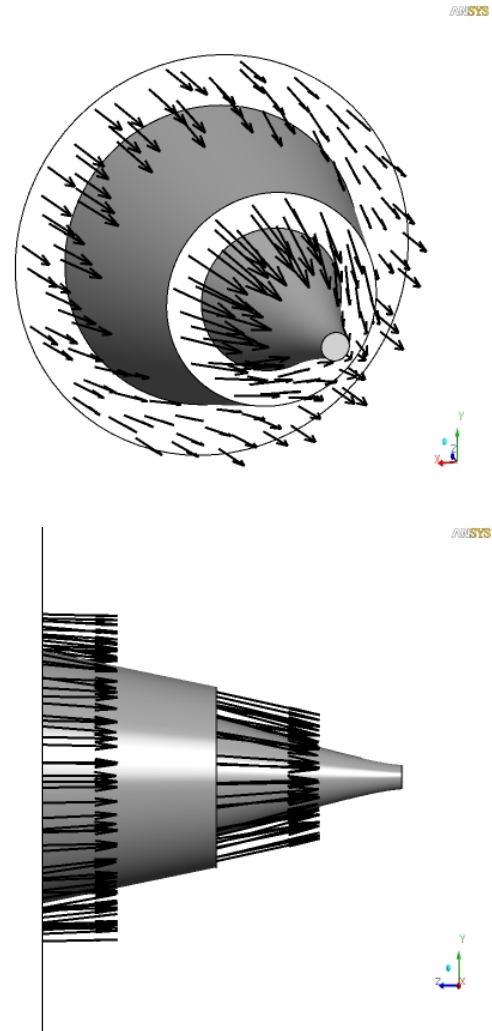


Fig. 7. Velocity vector orientation at the exhaust and bypass duct exits.

The boundary conditions at the lateral cylindrical boundary of the calculation domain were set as "opening" with specifying the velocity vector and the temperature as in the free stream ($V_x = 0$, $V_y = 0$, $V_z = -216$ m/s, $T = 223.15$ K).

The boundary conditions at all other boundaries (the temperature and total pressure at the inlet boundary, the pressure of the undisturbed flow at the outlet boundary, the tangency conditions together with the "no-slip wall" and adiabatic conditions at the nozzles surface) were given similar to the problem of wake simulation from the section 2.1.

3.2 Numerical results

Calculations were performed using ANSYS CFX soft. Comparison of the results obtained on different grids, showed that calculations on grids with 1 and 6 million cells gave very close fields of flow parameters due to adaptation of grids in both cases to the boundaries of the computational domain and flow structure. Below the results for the case of 1 million cells grid are presented.

At the annular exhaust duct exit were chosen 7 points, uniformly distributed in the radial direction, and flow parameters along streamlines originating from these points were calculated. The view of these streamlines is illustrated in Fig. 8. Further there will be shown distributions of gas-dynamic parameters along these seven streamlines.

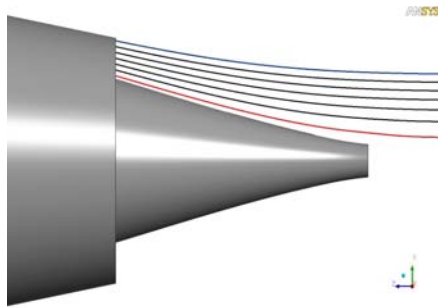


Fig. 8. Side view of the nozzles exits and streamlines, originating from different points of the exhaust duct outlet.

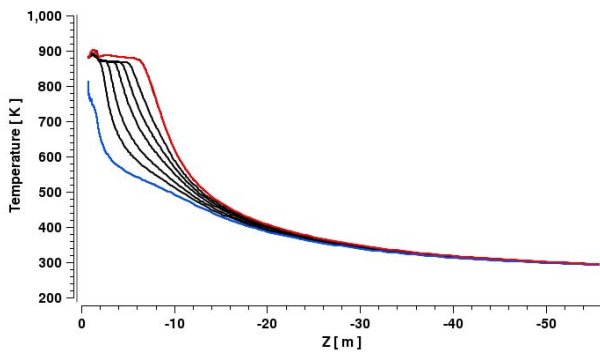


Fig. 9. Distribution of temperature along seven streamlines, illustrated in the Fig. 8.

Fig. 9 displays the distribution of temperature along mentioned 7 streamlines (see Fig. 8). It is seen that near the nozzle exit the temperature distribution across the flow is

extremely nonuniform. Along the streamline, which is closest to the periphery of the the exhaust duct jet, the temperature decreases more rapidly than the temperature along the streamline located closest to the axis of the flow. At the same time temperature along the last one remains very high at a distance of about 5 meters from the nozzle exit and only since $z = -6$ m begins to fall from 883.36 K to 295 K ($z = -55$ m). Downstream, the temperature distribution across the exhaust jet becomes almost uniform (the temperature along all streamlines is equalizing, tending to the same value).

Fig. 10 illustrates the kinetic turbulence energy distribution along the same streamlines. It is seen that the curves near the nozzle differ significantly from each other, and then (at the distance from about $z = -10$ m) they almost merge into a single curve. The kinetic energy of turbulence reflects the level of flow turbulence, which in the case of a turbofan engine reaches a maximum in the area of mixing jets from the exhaust and bypass ducts.

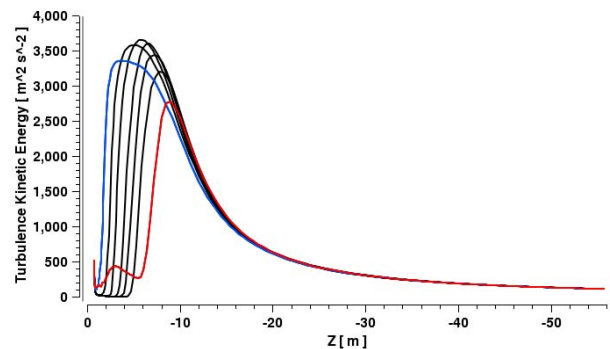


Fig. 10. Distribution of kinetic energy of turbulence along seven streamlines, illustrated in the Fig. 8.

In Fig. 11 is presented the field of temperature in (yz) - and (xz) -planes. As it was said earlier, the temperature distribution is of great importance for further calculations of water vapour condensation in the products of fuel combustion. It can be seen that the jet remains rather narrow along the considered distance from the nozzle exit. Field of temperature in the closest to the engine cross-section and at the outlet boundary also confirms this fact (Fig. 12). Recall that at the outer

lateral boundaries of the computational domain the undisturbed flow speed was set, and it was coincided with the speed of oncoming flow when an airplane cruising. Essentially, the propagation of a turbofan jet in a co-current flow was studied.

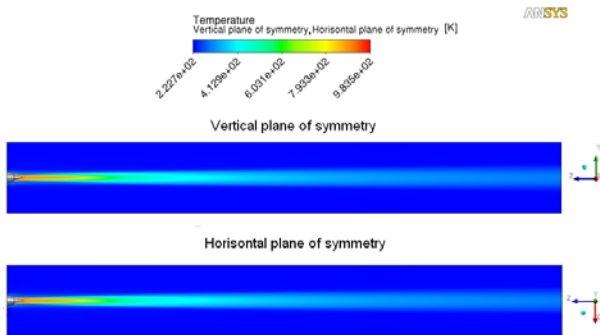


Fig. 11. Temperature fields in the vertical and horizontal planes of symmetry of the calculation domain.

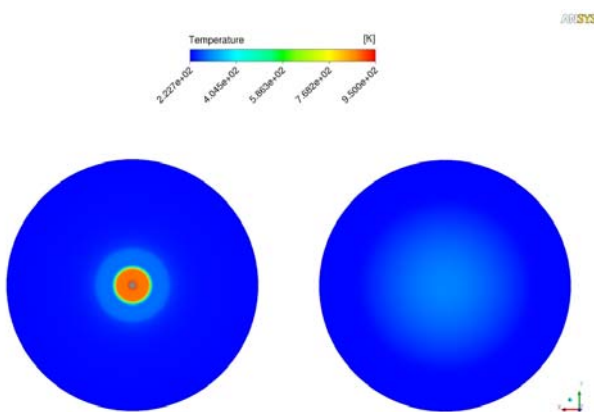


Fig. 12. Temperature field in two cross-sections of the jet.

4 Modeling of the initial stage of water vapour condensation in the exhaust jet

4.1 Description of the condensation model

In the present study all nucleation calculations have been done on the basis of condensation model «vapour-crystal» [8]. Its key principals and assumptions are:

1. Molecules of substance, in this case - water, are considered as simple, indivisible particles, which do not have internal structure and internal degrees of freedom. It allows avoiding needless detailed analyzation at the

interatomic level and, for example, to use averaged gas-kinetic cross-sections of objects, which in such setting of the problem are constants for monomers and described by a simple function for a cluster of any size. No physical and chemical transformations inside of molecules of water occur, but within the framework of a problem molecules can form between themselves or break off earlier created bonds of various intensities. Surrounding gases here play a role of an inert ambient.

2. The binding energy of molecules of a substance, which may be connected to a monomer or a previously created cluster (particle), increases with the particle size in accordance, e.g., with the results of [9]. When assembling dimer (two molecules cluster), this energy is equal to the dissociation energy. When connecting the molecule to a sufficiently large cluster, energy, equal to the heat of evaporation of the same molecule, releases. Between these two limiting cases there are several discrete values of the attachment energy, i.e. binding potentials, which may be implemented in different molecule's positions in clusters of different sizes and shapes. These potentials are determined by the thermal properties of the material [8, 10].

3. The rates of cluster assembly and disintegration depend on binding energy of already composed element, relative velocity of surrounding particles and probability of their collision.

The probability of collision is determined from the gas-kinetic cross-sections of objects and their mutual speed using a standard Maxwellian distribution for the thermal velocities. Besides, in calculations, velocity of the relative motion of relatively large particles in turbulent pulsations of the certain scale is considered.

4. The following algorithm determines probabilities of the acts of molecule attachment or detachment from the cluster during the impact interaction.

In the Maxwellian velocity distribution of the molecules impacting (colliding) with previously collected particles, is as a rule a fraction of molecules that can break off previously formed bond. Then during an impact

process, separation of a new molecule from a cluster is probable.

In the same Maxwellian distribution there are always molecules whose energy is small, less than the formation energy of a new, yet a vacant bond. In case of contact of such low-speed molecules with free surface there is a probability of their attachment and the cluster size increase.

If the energy of the molecule colliding with the cluster is more than energy of attachment with the formation of a new bond, and less than earlier bond dissociation energy, the most probable outcome of collision will be an ordinary elastic energy exchange.

Threshold values, i.e. bond potentials for each particle are known. The fraction of surrounding molecules in the Maxwell distribution, which are capable to participate (for these values of potentials) in either growth of the cluster, or destruction of its preformed bonds, or – only able to an elastic thermal energy exchange, are also known. In sum, the data is sufficient for describing the dynamics of the phase transitions with the particles of arbitrary shape and size.

5. Beside the process of molecules separation from the cluster under the influence of external impact, the internal evaporation process is also considered. Its rate depends on the ratio of the same bond potentials and energy of thermal fluctuations of molecules, which is determined by the current temperature.

As to assembly of structures from the crystals, the fundamental change of the model is not required. The amendments relate only to a form of a developed structure and methods of taking into account their cross-sections in collisions.

The elementary processes energy was set by the following row of the resolved potential levels of interaction between molecules of water: $\varphi_1 = 0.25$ eV, $\varphi_2 = 0.07$ eV, $\varphi_3 = 0.058$ eV, $\varphi_4 = 0.024$ eV. Potential values are assigned in accordance with the principles given in [8, 10]. Generalized binding energy in the volume $\varphi_V = 0.42$ eV, and on the surface of the particles $\varphi_H = (0.42 - 0.055) = 0.37$ eV

were taken into account. On the basis of these values, an approximating relation was constructed for the energy of monomer attachment to a cluster, depending on the size of the latter, similar to a relation used in the Bauer paper [9].

The advantage of this model is the opportunity of the condensation analysis and calculation at any stage of the process, determination of small concentrations of molecular complexes without the use of the equilibrium ratios, without the concepts of the critical nucleus and liquid phase surface tension forces.

The essential feature of this approach is more detailed account of the probability of separation of single molecules (monomers) from the cluster. It is used quasi-Boltzman distribution of water molecules, bounded at the surface, in their resolved energy states. It is added by the determination of the recovery frequency distribution through the frequency of thermal fluctuations and effective value of probability of the resolved transition.

Serious difference of the proposed scheme from the classical nucleation theory (CNT) is that we managed to find and apply an enough adequate mechanism of accounting collisions between clusters. The frequency of such collisions, as a rule, is considered to be small, and the growth rate of particles of the present mechanism is neglected in comparison with the speed of exchange of monomers with vapour. For this reason, collisions between clusters are not included in the condensation gas-dynamic processes [11, 12, 13]. Careful analysis of the effective rate of drops merging shows that it can appear essential if the individual reaction of a cluster with any other cluster is not taken into account, but the total effect of the interaction of particles of a particular size with the total aggregate of the condensed particles. Total mass growth rate in this case is comparable by effectiveness with the common mechanism of interaction with the monomers.

4.1 Results of condensation modeling

One of the most important results of calculations of water vapour condensation in

the turbofan jet in a co-current flow are graphics, presented in Fig. 13 and Fig. 14. Both pictures are shown for the middle streamline (fourth in Fig. 8).

Consider the Fig. 13. Initially at the exhaust duct outlet there are only monomers, and small clusters begin to arise. In the picture, almost at the nozzle exit curves jumps can be seen. This indicates that at such parameters at the nozzle outlet (temperature 883 K, pressure of 28242 Pa) a certain number of particles with the number of molecules up to 7 are already formed. By the reason of interaction between them they create larger clusters, which due to the large surface begin to capture small clusters. The particle size increases and moves downstream with the jet cooling and temperature decreasing.

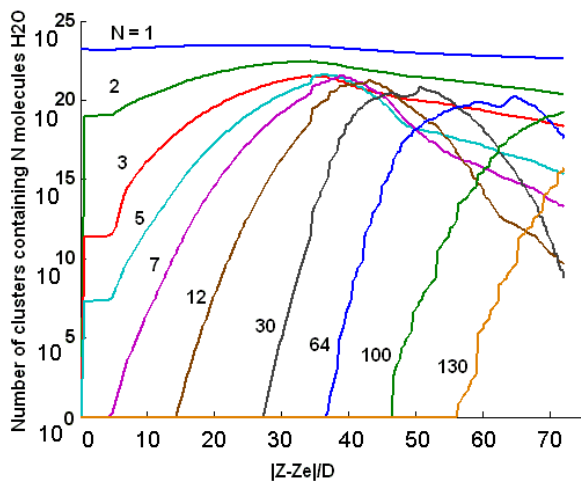


Fig. 13. Number of water clusters with N molecules versus relative distance from the engine nozzle. Z_e is the coordinate of the exhaust duct exit, $D=0,762$ m is the outer diameter of the annular exhaust duct outlet.

On the other hand, due to collisions with fast monomers from larger particles detached single molecules, which interact with each other, maintaining the concentration of small clusters. Also at the same distribution curve appears a gap in the concentration of medium-sized particles (Fig. 14).

As soon as the total surface of large clusters grows they capture medium clusters, whereby concentration of clusters of the average size tends to zero (in Fig. 14 this graph is not presented, but it should be noted that

even at large distances, the minimum at distribution curve goes down). Further, as a result of mutual collisions average size of large clusters is constantly increasing, and they actively take clusters of the middle region. This separation of monomers is no longer able to compensate this process, and the distribution more clearly divided into two: the distribution of small clusters and the distribution of small droplets.

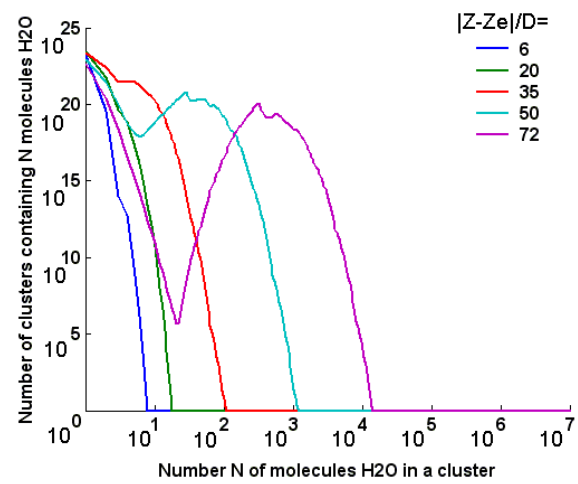


Fig. 14. Distribution of clusters in the number of molecules at different fixed relative distances from the nozzle. Z_e is the coordinate of the exhaust duct exit, $D=0,762$ m is the outer diameter of the annular exhaust duct outlet.

It is noteworthy that the observed peak appears over a fairly wide range of conditions, both at supersaturation and at low moisture, with the parameters that are far from the saturation curve.

5 Conclusions

In the present study a large-scale vortex structure in the near wake of an aircraft is investigated. The results of calculations in the framework of RANS-approach confirmed a reduction of the vortex drag of aircraft by winglets. At the same time contrary to the common view, winglets have a very slight effect on the formation of circulation flow arising on the wingtips.

The structure of flow in the exhaust stream of the turbofan engine CFM 56-3 and the initial

stage of condensation of water vapour in the products of fuel combustion are investigated. Three-dimensional (not axisymmetric) formulation of the problem was used. Jet stream was modeled on structured block grid with different total number of cells (1, 6, and 10 million cells). Analysis of simulation results allowed determining the grid parameters to ensure an acceptable accuracy of jet simulation at a relatively small number of grid cells. It appeared that 1 million cells is sufficient for the simulation of the temperature distribution in the stream with high accuracy.

The calculations of the initial stage of condensation of water vapour in the turbofan jet flow allowed obtaining distributions of water clusters in size along and across the jet. A physical interpretation of the results is given.

Acknowledgements

This work was supported by Russian Foundation for Basic Research (grant No. 12-08-01282). The author thanks Professor Yu. M. Tsirkunov for his attention to this work, help in setting up the problem, and discussions of numerical results.

References

- [1] Report of the High Level Group on Aviation Research. *Flightpath 2050. Europe's vision for aviation*. Luxembourg: Publications office of the European Union, 2011.
- [2] <http://www.cleansky.eu/>
- [3] <http://www.b737.org.uk/>
- [4] http://www.ae.illinois.edu/m-selig/ads/coord_database.htm
- [5] Menter F.R. Two-equation eddy-viscosity turbulence models for engineering applications. *AIAA Journal*, Vol. 32, No. 8, pp. 1598–1605, 1994.
- [6] Menter F.R., Kuntz M. and Langtry R. Ten years of industrial experience with the SST turbulence model. *Turbulence, Heat and Mass Transfer 4* (Eds.: K. Hanjalic, Y. Nagano and M. Tummers). Begell House, 2003.
- [7] Lobanova M.A., Tsirkunov Y.M. Numerical simulation of a jet-vortex wake behind a cruise aircraft. *CD-ROM Proceedings of the 6th European Congress on Computational Methods in Applied Sciences and Engineering (ECCOMAS 2012), September 10–14, 2012, Vienna, Austria*, Eds.:

- Eberhardsteiner, J.; Böhm, H.J.; Rammerstorfer, F.G., Publisher: Vienna University of Technology, Austria, paper No. 1823, 14 p, 2012.
- [8] Igolkin S.I. Condensation model vapor-crystal. *J. of Technical Physics*, Vol. 66, No. 9, pp. 1-11. [In Russian]
- [9] Bauer S.H., Frurip D.J. Homogenous Nucleation in Metal Vapors. 5. A Self-Consistent Kinetic Model – *J. Chem. Phys.*, Vol. 81, No. 10, pp. 1015-1024, 1977.
- [10] Gorbunov A.A., Igolkin S.I. Mathematical Simulation of Volumetric Growth of Clusters in Overcooled Vapor. *Proceedings of the Fourth International Conference "Single Crystal Growth and Heat & Mass Transfer" (ISCG-01)*, Obninsk, Russia, Vol. 4, pp. 931-939, 2001.
- [11] Gorbunov V.N., Pirumov U.G., Ryjov Yu.A. *Non-equilibrium condensation in high-speed gas flow*. Moscow, Mashinostroenie, 1984. [In Russian]
- [12] Chirichin A.V. Numerical study of non-equilibrium heterogeneous-homogeneous condensation in supersonic nozzles. *Izv. Akademii Nauk, USSR, Mekh. Zhidkosti i Gasa*, No. 12, 1977. [In Russian]
- [13] Senkovenko S.A., Stasenko A.L. *Relaxation processes in supersonic gas jets*. Moscow, Energoatomizdat, 1985. [In Russian]

Contact Author Email Address

Mailto: lbnv.spb@gmail.com

Copyright Statement

The authors confirm that they, and/or their company or organization, hold copyright on all of the original material included in this paper. The authors also confirm that they have obtained permission, from the copyright holder of any third party material included in this paper, to publish it as part of their paper. The authors confirm that they give permission, or have obtained permission from the copyright holder of this paper, for the publication and distribution of this paper as part of the ICAS 2014 proceedings or as individual off-prints from the proceedings.